J Appl Electrochem (2008) 38:663–668
DOI 10.1007/s10800-008-9489-3

ORIGINAL PAPER

Polarisation behaviour of Al–Zn–Ga alloy in chloride medium

D. O. Flamini · S. B. Saidman

Received: 29 August 2007 / Revised: 5 January 2008 / Accepted: 11 January 2008 / Published online: 9 February 2008

Abstract The electrochemical response of Al–Zn–Ga alloy in chloride medium was studied. For this purpose, linear sweep voltammetry and open circuit potential (OCP) measurements were employed and surface characterisation was performed by scanning electron microscopy (SEM) and energy dispersive X-ray (EDX) analysis. The presence of Ga whether as alloyed element in the ternary alloy or deposited from the electrolyte solution onto pure Al or onto Al–Zn alloy causes a displacement of the onset of the process of dissolution towards more negative potential in a chloride solution. The anodic behaviour of the Al–Zn–Ga alloy can be interpreted in terms of an amalgam mechanism, where the homogeneously distribution of Ga in the alloy assures the formation of a superficial Ga–Al amalgam.

Keywords Al–Zn–Ga alloy · Aluminium · Gallium · Activation mechanism · Amalgam

1 Introduction

Aluminium is unsuitable as a sacrificial anode in cathodic protection systems as well as anode material in batteries due to the spontaneous formation of a passivating oxide. The incorporation of alloying elements such as Hg, Zn, In and Ga is used to shift the potential towards sufficiently electronegative values. Some work has been conducted to study the effects imparted by Ga when alloyed with Al or when present as an ion in solution [1–4].

D. O. Flamini · S. B. Saidman (✉)
Instituto de Ingeniería Electroquímica y Corrosión (INIEC), Departamento de Ingeniería Química, Universidad Nacional del Sur, Av. Alem, 1253, 8000 Bahia Blanca, Argentina
e-mail: ssaidman@criba.edu.ar

There is general agreement that Ga accelerates anodic dissolution of Al and several mechanisms have been proposed to account for this. It has been suggested that Ga allows chloride adsorption at more negative potentials [3, 4]. It has also been proposed that Ga particles at the metal/oxide interface cause local thinning of the passive oxide film [1]. In a previous paper an amalgam-activation mechanism was proposed which needs a minimum amount of quasi-liquid Ga in true metallic contact with Al [5]. Gallium surface diffusion undermines and detaches the Al oxide, increasing the active area. Al oxidation at the amalgam/solution interface gives an active potential. The presence of Zn electrodeposited from the solution or as an alloying component assures that the critical surface concentration of Ga needed to activate is reached.

Although several studies have been carried out on the corrosion of Al–Zn–In alloys [6–8], the electrochemical behaviour of the Al–Zn–Ga alloy has received little attention [9]. Continuing the work on the activation process of Al in the presence of Ga and Zn, the electrochemical behaviour of the Al–Zn–Ga alloy is reported here. Potentiodynamic and open circuit potential (OCP) measurements are employed and surface characterisation is performed by scanning electron microscopy (SEM) and energy dispersive X-ray analysis (EDX). Electrochemical impedance spectroscopy (EIS) was used to comparatively study the corrosion behaviour of pure Al and Al–Zn in chloride media in the presence of Ga^{3+} with that of the ternary alloy.

2 Experimental details

Disc electrodes made from pure Al, Al–3.9%Zn and Al–5.6%Zn–3.0%Ga alloys embedded in a Teflon holder were used as working electrodes. Alloys were obtained

using pure metals (99.99%, Aldrich Chemical Co.). The discs were polished with 1000 grit SiC emery paper followed by 1 μm and 0.3 μm grit alumina suspensions and then cleaned with triply distilled water. The auxiliary electrode was a large Pt sheet. Potentials were measured against a SCE reference electrode connected through a Luggin–Haber capillary tip and are thus given throughout this work.

Linear sweep voltammetry at 0.005 V s^{-1}, initiating at the more negative potential, were applied to electrodes either still or under rotation. Electrochemical experiments were carried out using a potentiostat–galvanostat (PAR Model 273 A) and a potentiostat–galvanostat (Voltalab 40 Model PGZ 301). A dual stage ISI DS 130 SEM and an EDAX 9600 quantitative energy dispersive X-ray analyser were used to examine the electrode surface characteristics. Ac impedance spectra were recorded when the open circuit potential was stabilised, using an excitation voltage of 10 mV. The frequency range studied was between 10 kHz and 10 mHz.

Chloride solutions (0.5 M NaCl) containing 0.01 M Ga^{3+} were prepared and the pH was adjusted to 2.5 with HCl. All chemicals were reagent grade and solutions were freshly made in triply-distilled water. Measurements were performed in a purified nitrogen gas saturated atmosphere.

3 Results and discussion

The voltammogram of Al–Zn–Ga in 0.5 M NaCl, pH 2.5 solution between −2 V and −1.2 V at 0.005 V s^{-1} is presented in Fig. 1, curve a. A current peak can be observed at the more negative potentials. This peak may be due to the summation of hydrogen evolution and Al dissolution which occur at the same electrode potentials [10]. At more positive potentials, a passive region is observed followed by a sharp current increase. The anodic current begins at −1.36 V, consistent with the OCP (Fig. 2a). The active behaviour initiates practically at the same potential in the pH range

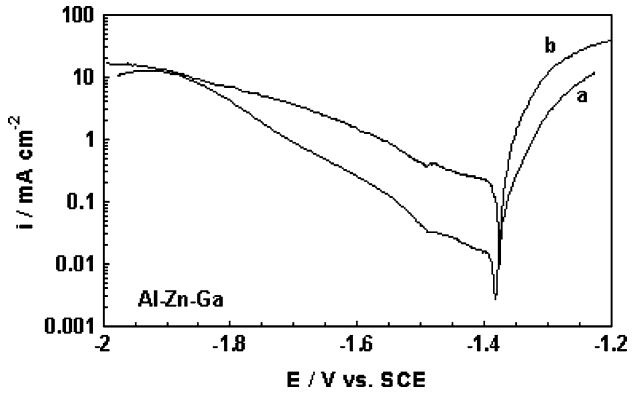

Fig. 1 Voltammogram of Al–Zn–Ga alloy at 0.005 V s^{-1} in a 0.5 M NaCl, pH 2.5 solution at 25 °C: (a) without Ga^{3+} and (b) with 0.01 M Ga^{3+}

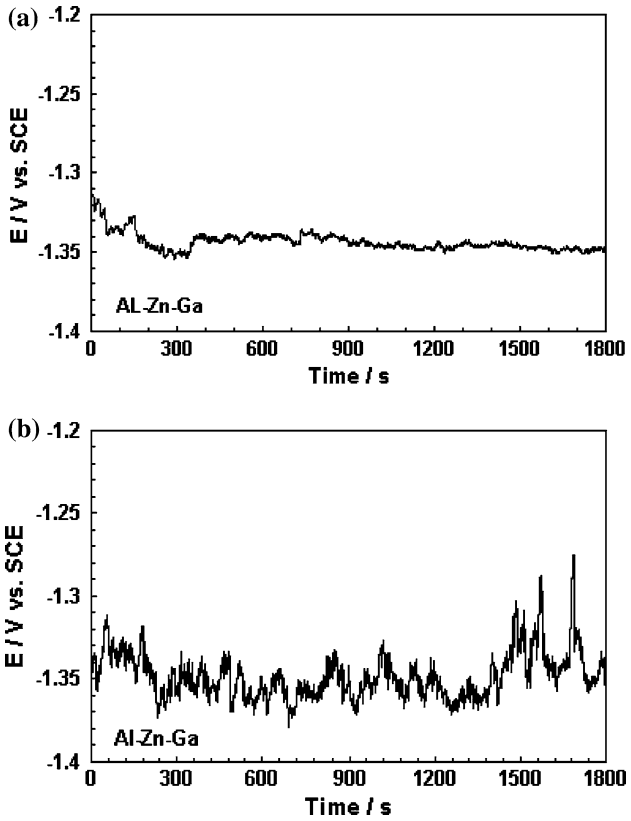

Fig. 2 Open circuit potential vs. time plot of Al–Zn–Ga alloy in a 0.5 M NaCl, pH 2.5 solution at (**a**) 25 °C and (**b**) 60 °C

2.5 ≤ pH ≤ 6. The response corresponding to the Al–Zn–Ga alloy in the presence of Ga^{3+} is also included (Fig. 1, curve b). An increased cathodic current is measured which is associated with the deposition of Ga. Although the anodic current initiates at practically the same potential as in the absence of the activator, the anodic dissolution is significantly depolarised when Ga^{3+} is added to the solution.

The influence of temperature was also analysed. It was found that the OCP vs. time plot (Fig. 2b), as well as the voltammogram (Fig. 3) at 60 °C in a 0.5 M NaCl, pH 2.5

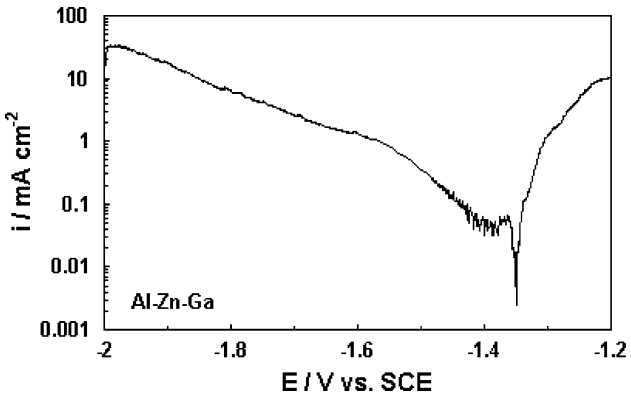

Fig. 3 Voltammogram of Al–Zn–Ga alloy at 0.005 V s^{-1} in a 0.5 M NaCl, pH 2.5 solution at 60 °C

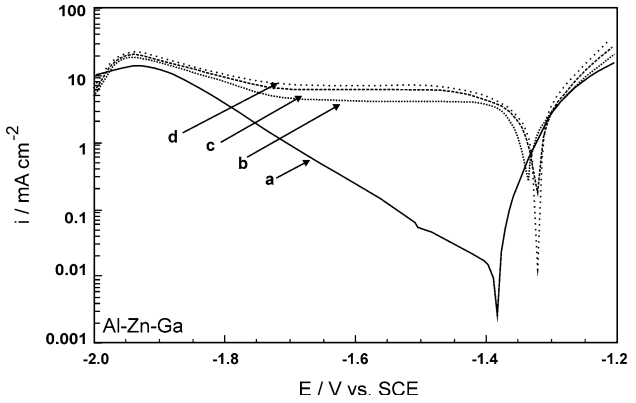

Fig. 4 Voltammogram of Al–Zn–Ga alloy at 0.005 V s^{-1} in a 0.5 M NaCl, pH 2.5 solution at different rotation rates: (a) 0 rpm, (b) 500 rpm, (c) 1000 rpm and (d) 1500 rpm

solution, are almost identical with those obtained at 25 °C. In the case of Al–Zn–In it is postulated that the exothermic hydrolysis reaction of the Al^{3+} ions provides a sufficiently high temperature to promote the presence of quasi-liquid In [8]. This fact and the low melting point of Ga explain the independence of the electrochemical behaviour of the Al–Zn–Ga alloy with solution temperature.

If the electrode is rotated during the potential scan the shape of the polarisation curve is similar to that obtained without rotation but higher currents, both anodic and cathodic, are measured as the rotation rate increases (Fig. 4). Moreover, the corrosion potential is independent of the rotation rate.

Figure 5 shows the SEM/EDX examination of the ternary alloy surface polarised from −2 V to −1 V at a scan rate of 0.005 V s^{-1}. The attacked areas are uniformly distributed (Fig. 5a). A close view of these areas shows irregular, non-crystallographic, probably tunnel-like pits (Fig. 5b). This morphology is similar to that found for the Al–Zn alloy [11], although for the ternary alloy investigated here pits are not deep. Moreover, the cavities are covered with a cracked film. In the case of the Al–Zn–In alloy the attack initiates and propagates in those zones enriched in In and Zn during the solidification process, i.e., grain boundaries and interdendritic zones [8]. The low solubility of In in the Al matrix according to the binary alloy phase diagrams (0.19 wt% In) explains this segregation [12]. Conversely, the higher solubility of Ga in Al (2 wt%) [12] explains the homogeneous distribution of the attacked areas. The more uniform pitting distribution ensures higher current efficiency, which constitutes a requirement for a sacrificial anode. EDX analysis performed inside the damaged areas (Fig. 5c) showed increasing amounts of Ga (7.72 wt%) and Zn (18.83 wt%) compared to the rest of the electrode surface (Fig. 5d). This accumulation indicates that preferential Al dissolution takes place in the attacked area.

The average corrosion potential of the ternary alloy under study in acid chloride solution (−1.34 V) indicates an active

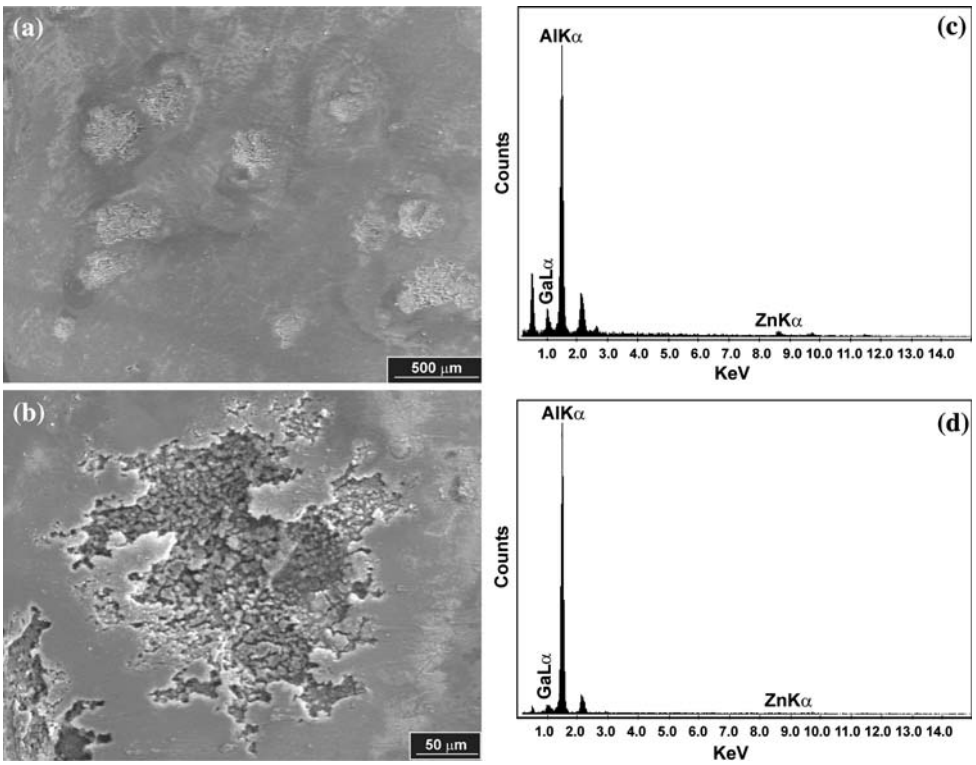

Fig. 5 (**a**) SEM micrograph showing the attacked areas uniformly distributed onto electrode surface of Al–Zn–Ga alloy, (**b**) magnified SEM image of the attacked area, (**c**) EDX spectrum inside of the attacked area and (**d**) EDX spectrum outside of the attacked area

state. A nominal composition of 2.6% Ga was used because this percentage assures an activated Al–Ga alloy [13]. The onset of anodic currents in the i/E curve of the ternary alloy presented in Fig. 1 practically matches that of the Al–Zn alloy in the presence of Ga^{3+}. Figure 6 shows the voltammogram in the anodic direction at 0.005 V s^{-1} for an Al–Zn alloy after different polarisation times at −2 V. The voltammetric curves show an anodic peak which is attributable to an activation process by amalgam depassivation control [5], where Al incorporation and diffusion within the amalgam is followed by its oxidation at the amalgam/solution interface. The agreement between the onsets of the anodic currents for both systems suggests that in the case of the ternary alloy the Ga–Al amalgam is also responsible for activation. The presence of Ga as an alloying component promotes and maintains the active state. At higher anodic potentials, around −1.1 V, the presence of Ga facilitates chloride adsorption and then the pitting process ensues.

For a better assessment of the activation process additional information was obtained by using EIS. The Nyquist diagram for the ternary alloy without electrode rotation shows a slightly depressed semicircle followed by a tail in the low frequency range (Fig. 7, curve a). In principle the impedance spectra in the high frequency range can be interpreted by a simple Randles circuit comprising a parallel combination of a resistor representing the charge-transfer resistance (R_{ct}) and a capacitor representing the electrode capacitance (C), in series with a resistor representing the ohmic drop in the electrolyte solution. (R_s). The R_{ct} is directly associated with the rate of the electrochemical corrosion reaction [14]. Because of the low value of R_s, R_{ct} can be determined by extrapolation of the semicircle up to the real axis. The semicircle depression in the Nyquist plot is attributable to surface heterogeneity and/or roughness.

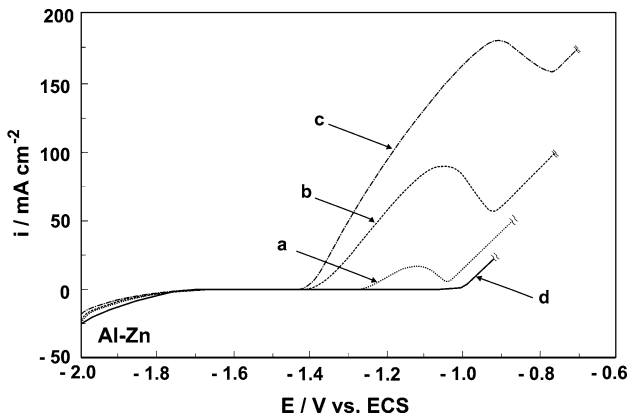

Fig. 6 Voltammogram of Al–Zn alloy at 0.005 V s^{-1} in a 0.5 M NaCl, pH 2.5 solution with 0.01 M Ga^{3+} at different cathodic polarisation times at −2.0 V: (a) 60 s, (b) 600 s and (c) 1200 s. The voltammogram of Al–Zn alloy in a 0.5 M NaCl, pH 2.5 solution without Ga^{3+} after cathodic polarisation at −2.0 V during 10 min is also included (curve d)

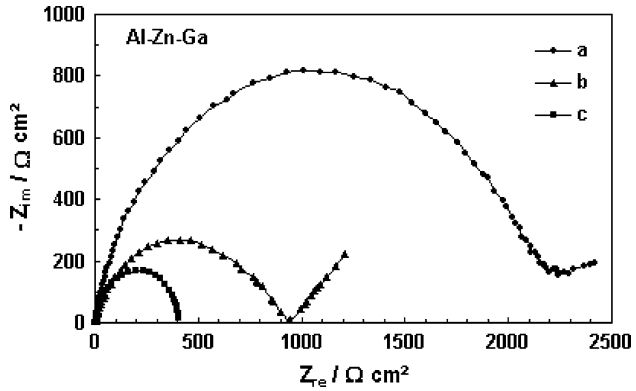

Fig. 7 Nyquist plots for Al–Zn–Ga alloy at open circuit potential condition in a 0.5 M NaCl, pH 2.5 solution: (a) without Ga^{3+}, (b) with 0.01 M Ga^{3+} and (c) without Ga^{3+} under electrode rotation (500 rpm)

According to Fig. 7, curve a, R_{ct} is 2.21 kΩ cm^2 and is smaller in the presence of Ga^{3+} (0.9 kΩ cm^2) (Fig. 7, curve b) demonstrating that Ga^{3+} causes enhanced corrosion. When Ga^{3+} is dissolved in solution, greater amounts of the metal are deposited facilitating amalgam formation.

Under rotation the impedance of the Al–Zn–Ga alloy in chloride solution reduces to a semicircle with diameter equal to 0.4 kΩ cm^2 (Fig. 7, curve c) indicating a higher corrosion rate compared with that obtained under stagnant conditions. This result agrees with that obtained under potentiodynamic polarisation.

To gain a better understanding of the role of Ga and Zn on the corrosion behaviour of Al, impedance data were obtained for Al and Al–Zn electrodes in chloride solution with and without addition of the activator. The effect of varying the cathodisation time at −2.0 V on the polarisation behaviour of Al in chloride solution containing Ga^{3+} was first analysed (Fig. 8). The pitting process initiates at

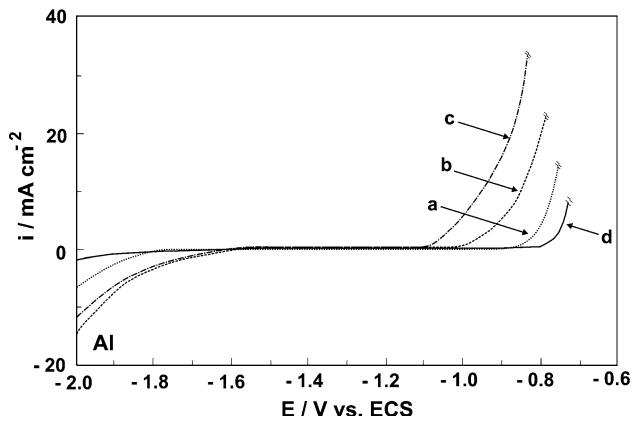

Fig. 8 Voltammogram of pure Al at 0.005 V s^{-1} in a 0.5 M NaCl, pH 2.5 solution with 0.01 M Ga^{3+} at different cathodic polarisation times at −2.0 V: (a) 60 s, (b) 600 s and (c) 1200 s. The voltammogram of pure Al in a 0.5 M NaCl, pH 2.5 solution without Ga^{3+} after cathodic polarisation at −2.0 V during 10 min is also included (curve d)

more negative potentials as the cathodisation time increases because higher amounts of Ga are deposited. A decrease in the semicircle diameter is observed when the Al electrode is held at −2.0 V (Fig. 9, curves a and b). This is explained by the oxide hydration/elimination by local alkalinisation produced during hydrogen evolution on the Al surface. On the other hand, there are clear differences between the Nyquist plot obtained for bare Al and for the Al electrode with deposited Ga after cathodisation (Fig. 9, curves b and c). R_{ct} is reduced by almost an order of magnitude in the presence of deposited Ga, which is consistent with enhanced Al dissolution sustained by chloride adsorption produced by the presence of Ga at more negative potentials [3, 4, 15].

Figure 10 illustrates the EIS data of Al–Zn alloy with and without the activator. The overall impedance is significantly smaller for the alloy compared with that obtained for pure Al in agreement with enhanced Al dissolution in the presence of Zn [11, 16]. The Nyquist plot for the Al–Zn alloy in chloride solution shows two capacitive loops. The R_{ct} increases when Ga is deposited

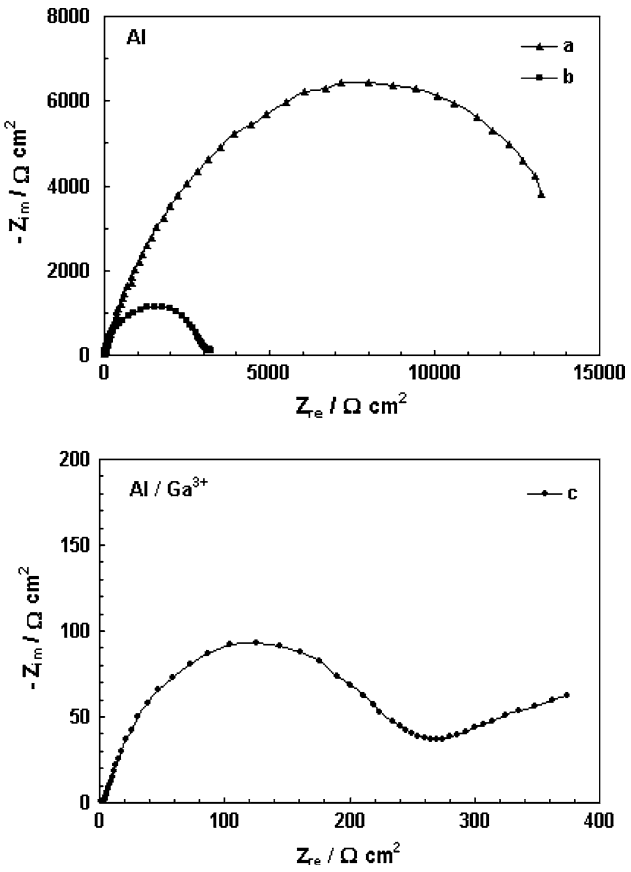

Fig. 9 Nyquist plots for pure Al at open circuit potential condition in a 0.5 M NaCl, pH 2.5 solution: (a) without previous cathodisation, (b) after cathodic polarisation at −2.0 V during 10 min and (c) after cathodic polarisation at −2.0 V during 10 min in the presence of 0.01 M Ga^{3+}

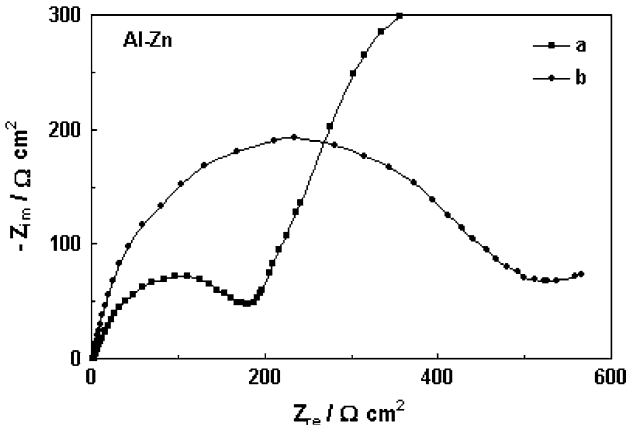

Fig. 10 Nyquist plots for Al–Zn alloy at open circuit potential condition in a 0.5 M NaCl, pH 2.5 solution after cathodic polarisation at −2.0 V during 10 min: (a) without Ga^{3+} and (b) with 0.01 M Ga^{3+}

onto the binary alloy. The reason for this change can be explained considering that different mechanisms are operative and consequently, different corrosion rates are expected. As already mentioned, the oxidation mechanism of the bare alloy is a chloride pitting process while it is possible to activate Al–Zn alloy via Ga–Al amalgam formation that occurs at more negative potentials. On the other hand, it is reasonable to suppose that the true electrochemically active areas are different for both processes.

The appearance of the second capacitive loop at the low frequency values in the plot corresponding to the binary Al–Zn alloy may be related to the precipitation of $Zn(OH)_2$ on the electrode surface [17]. It is reasonable to assume the same for the Al–Zn–Ga alloy, considering the similarities between the diagrams from the binary and ternary alloys. The suppression of the second capacitive loop under electrode rotation for the ternary alloy (Fig. 7, curve c), supports this because, in this case, corrosion product accumulation is hindered. Likewise, polarisation resistance is reduced under rotation, and this decrease is attributable to the difficulty in forming protective corrosion products.

4 Conclusions

Activation of the Al–Zn–Ga alloy investigated takes place at potentials where adsorption of chloride is not feasible. This process can be interpreted in terms of an amalgam mechanism. The alloyed Ga homogeneously distributed assures the formation of the Ga–Al amalgam. The attacked areas are uniformly distributed and are not deep. The material is able to provide higher currents when the amount of Ga deposited at the interface is increased by electrodeposition from the solution. Accumulation of corrosion products is reduced under rotation, giving higher corrosion rates.

EIS measurements allowed comparison of the activating effect exerted by Ga and Zn on the electrochemical behaviour of Al and confirmation of the mechanisms outlined previously for activation. The corrosion currents for the ternary alloy as well as for the Al–Zn alloy with Ga deposition are smaller than that of the bare Al–Zn alloy. This may be explained considering that the oxidation reaction changes from an amalgam-controlled dissolution to a pitting process.

Acknowledgments Financial support by the Secretaría de Ciencia y Técnica-UNS (PGI 24/M093/04) and the Consejo Nacional de Investigaciones Científicas y Técnicas (CONICET- PIP02143/00) is gratefully acknowledged.

References

1. Tuck CDS, Hunter JA, Scamans GM (1987) J Electrochem Soc 134:2970
2. Mance A, Cerović D, Mihajlović A (1985) J Appl Electrochem 15:415
3. Breslin CB, Carroll WM (1992) Corros Sci 33:1735
4. El Shayeb HA, Abd El Wahab FM, Zein El Abedin S (2001) Corros Sci 43:643
5. Flamini DO, Saidman SB, Bessone JB (2007) Thin Sol Films 515:7880
6. Breslin CB, Friery LP, Carroll WM (1994) Corros Sci 36:85
7. Venugopal A, Angal Rd, Raja VS (1996) Corrosion 52:138
8. Muñoz AG, Saidman SB, Bessone JB (2002) Corros Sci 44:2171
9. Aragon E, Cazenave-Vergez L, Lanza E, Giroud A, Sebaoun A (1997) Brit Corros J 32:263
10. Tomcsányi L, Nagy Zs, Somlai J, Borszéki J (1993) Electrochim Acta 38:2541
11. Muller IL, Galvele JR (1977) Corros Sci 17:995
12. Baker H (1992) ASM handbook, vol 3. Alloy phase diagrams, Ohio
13. Breslin CB, Carroll WM (1992) Corros Sci 33:1735
14. Rosalbino F, Angelini E, Macciò D, Saccone A, Delfino S (2007) Electrochim Acta 52:7107
15. Flamini DO, Saidman SB, Bessone JB (2006) Corros Sci 48:1413
16. Sato F, Newman RC (1999) Corrosion 55:3
17. Shibli SMA, George S (2007) Appl Surf Sci 253:7510